Density Functional Theory Study of Free-Radical Polymerization of Acrylates and Methacrylates: Structure−Reactivity Relationship

I. Değirmenci, D. Avcı, and V. Aviyente*

Chemistry Department, Boğazici University, 34342, Bebek, Istanbul, Turkey

K. Van Cauter, V. Van Speybroeck, and M. Waroquier

Center for Molecular Modeling, Ghent University, Proeftuinstraat 86, 9000 Gent, Belgium

Received May 16, 2007; Revised Manuscript Received September 28, 2007

ABSTRACT: Radical polymerization processes occur through a complex network of many different reactions. It is well-known that the polymerization rate is directly related to the monomer structure. The experimental polymerizability behavior is expressed as $k_p/k_t^{1/2}$, where k_p is the rate coefficient of propagation and k_t is the rate coefficient of termination. In this study, the reactivity of a series of acrylates and methacrylates is modeled in order to understand the effect of the pendant group size, the polarity of a pendant group, and the nature of the pendant group (linear vs cyclic) on their polymerizability. The geometries and frequencies are calculated with the B3LYP/6-31+G(d) methodology whereas the energetics and kinetics of these monomers have been studied using the two-component BMK/6-311+G(3df,2p)//B3LYP/6-31+G(d) level of theory. For rotations about forming/breaking bonds in the transition state, an uncoupled scheme for internal rotations has been applied with potentials determined at the B3LYP/6-31+G(d) level. Generally the rate constants for propagation k_p mimic the qualitative polymerization trend of the monomers modeled and can be used with confidence in predicting the polymerizability behavior of acrylates. However in the case of 2-dimethylaminoethyl acrylate, chain transfer is found to play a major role in inhibiting the polymerization. On the other hand, the disproportionation reaction turns out to be too slow to be taken into consideration as a termination reaction.

Introduction

Radical polymerization processes are complex since they involve many different reactions.[1] In a simple homopolymerization reaction, initiation, propagation, and termination steps occur and the propagating species may undergo a variety of chain transfer processes. The absolute and relative rates of these individual steps govern the overall rate of polymerization, the molecular weight, and the chain architecture. The ability to measure the rates of these individual reactions and the study of reaction mechanisms are extremely important and instructive as they lead to the development of accurate kinetic models and better methods for controlling the free-radical polymerization. Computational quantum chemistry has become a powerful tool to study directly the individual reactions within a complex process and to extract accurate mechanistic information such as geometries and relative rates of the elementary reactions.[2]

Photoinitiated polymerization of acrylates and methacrylates is used for the rapid production of polymeric cross-linked materials with defined properties. It is widely employed in the performance applications where emphasis is put on the mechanical as well as the optical properties. These applications are typically dental restorative fillers, fiber-optic coatings, optical adhesives, aspherical lenses for CD applications, and contact lenses.[3] In a typical formulation, acrylated multifunctional oligomers and small molecule monofunctional and multifunctional acrylates are used to adjust viscosity, rate of curing, and final film properties.

The polymerization rate is directly related to the monomer structure. The relationship between monomer structure and reactivity was investigated extensively in the late 1980s and 1990s by Decker et al. using several model monofunctional acrylates with various pendant groups ranging from cyclic carbonates and oxazolidones to dioxolanes and oxetanes.[4] Comprehension of the influence of molecular structure on acrylate reactivity has been sought ever since the first publications with acrylates and methacrylates. Decker's report on acrylates with a very high intrinsic reactivity assigned importance to hydrogen bonding as a potential reason for high rates of polymerization R_p.[5] Andrzejewska reported a heteroatom effect in the side chain which led to higher reactivity.[6] Hoyle et al. have investigated the relationship between the photopolymerization rate of hydroxyalkyl acrylates and their structure.[7] The photopolymerization rates of hydroxyalkyl acrylates are higher than those observed for typical monofunctional acrylate monomers and rival those of multifunctional monomers. However, even though the photopolymerization practice is well established, there are still limitations to this process. These limitations include residual unsaturation, oxygen inhibition, polymerization speed, and polymer properties. A typical method to increase the polymerization rate is to utilize monomers with more than one vinyl group. With an increase in the monomer functionality, diffusion limitations are encountered earlier in the polymerization and termination is also hindered earlier. This early reduction in termination leads to stronger autoacceleration and greater polymerization rates. These highly cross-linked materials have increased moduli; they are hard and brittle. However, increasing the cross-linking density leads to the residual unsaturation. The tradeoff between polymerization rate and residual unsaturation is important for the development and selection of monomers for use in polymerization applications. There is a desire to counteract these limitations and develop monomers that polymerize to a higher extent of reaction with greater polymerization rates.[8]

* Corresponding author.

10.1021/ma071106i CCC: $37.00
Published on Web 11/29/2007

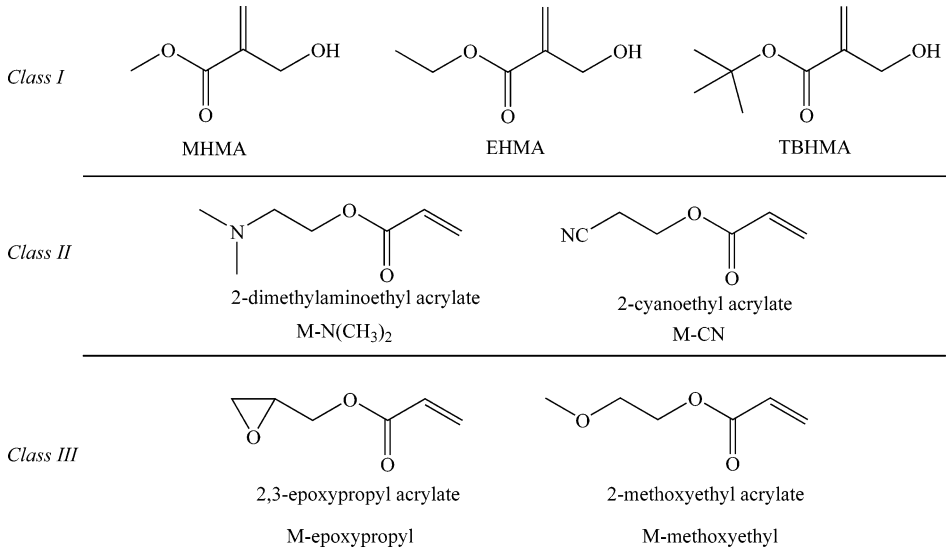

Figure 1. Monomers considered in this study.

Table 1. Experimental Rates of Polymerization (R_p) of the Substituted Acrylates and Methacrylates Modeled in This Study

no.	name	R_p (mol $L^{-1}s^{-1}$)	T (K)
M1	methyl α-hydroxymethacrylate (MHMA)	3.70×10^{-2} [a]	303.15
M2	ethyl α-hydroxymethacrylate (EHMA)	3.00×10^{-2} [a]	303.15
M3	*tert*-butyl α-hydroxymethacrylate (TBHMA)	1.60×10^{-2} [b]	303.15
M4	2-dimethylaminoethyl acrylate (M−$N(CH_3)_2$)	1.04×10^{0} [c]	298.15
M5	2-cyanoethyl acrylate (M−CN)	13.90×10^{0} [c]	298.15
M6	2,3-epoxypropyl acrylate (M−epoxypropyl)	4.11×10^{0} [c]	298.15
M7	2-methoxyethyl acrylate (M−methoxyethyl)	2.67×10^{0} [c]	298.15

[a] Reference 12. [b] References 12 and 14. [c] Reference 3a.

The reactivity of a series of acrylates was determined experimentally by Jansen et al. and a relation was found with the degree of hydrogen bonding as well as with the polarity of the monomer.[3] Lee et al. studied the influence of hydrogen bonding for hydroxyalkyl acrylates specifically because these systems show a behavior that differs from conventional acrylates, a decrease of polymerization rate with increasing temperature has been observed.[7] They presumed that the termination rates are greatly reduced by hydrogen bonding when polymerizing at lower temperatures, leading to an enhanced polymerization rate. In the mid 80s, the radical homopolymerization and copolymerization behavior of methacrylic esters containing heteroatoms at the α-position of alkyl groups have been investigated to elucidate the effects of structures on reactivity.[9] These investigations have revealed that the introduction of a heteroatom into the methyl group increases the reactivity of these monomers due to polar effects. The first such monomer investigated is that containing the hydroxymethyl group at the α-position, ethyl α-hydroxymethacrylate (EHMA).[9c]

Recently, some of the current authors published an ab initio study on the free radical polymerization of acrylates and phosphoacrylates in order to understand the mechanistic behavior of their free radical polymerization reactions.[10] Furthermore the different factors controlling the reactivity of a large series of carbon-centered radicals toward the methyl acrylate monomer were examined computationally by Lalevee et al.[11]

In this study, the structure−reactivity relationship of three different classes of acrylates has been investigated on an ab initio basis using density functional theory (DFT) with the aim of elucidating the effect of alkyl, polar, and cyclic pendant groups on their polymerizabilities. Elementary steps corresponding to propagation, disproportionation, and chain transfer have been studied.

The first class of acrylates aims to investigate the effect of pendant group size on the polymerizability. Mathias et al. have been pursuing the chemistry of α-hydroxymethacrylate (HMA) derivatives for several years.[12] Alkyl α-hydroxymethacrylates (RHMA) derivatives give faster photopolymerization rates than typical methacrylates.[13] In this study, the free radical polymerizabilities of a series of alkyl α-hydroxymethacrylates (methyl α-hydroxymethacrylate (MHMA), EHMA, and *tert*-butyl α-hydroxymethacrylate (TBHMA)) are investigated in an attempt to analyze in detail the effects exerted by the bulky groups on their polymerizabilities. Experimentally, it is known that α-substituted methacrylate MHMA polymerizes faster than EHMA and TBHMA.[13,14]

A second class of monomers investigates the effect of polar groups on the polymerizability of acrylates. More specifically the effect of an electron withdrawing (−CN) and an electron donor group (−$N(CH_3)_2$) on the polymerizability of acrylates is studied. It is known experimentally that 2-cyanoethyl acrylate (M−CN) polymerizes 13 times faster than 2-dimethylaminoethyl acrylate (M−$N(CH_3)_2$), and modeling is expected to shed light on this issue.[3a]

Finally in the third class, the effect of cyclic pendant groups in acrylates is modeled by comparison of a cyclic ether (2,3-epoxypropyl acrylate) with a straight-chain ether (2-methoxyethyl acrylate) since the former is known to polymerize twice as fast as the latter.

The three classes of acrylates are shown in Figure 1. The experimentally determined rates of polymerization (R_p) of the various monomers are summarized in Table 1.

Methodology

1. Reaction Mechanism of Free Radical Polymerization. The free-radical polymerization proceeds via a chain mechanism, which basically consists of four elementary reactions, i.e., initiation, propagation, chain transfer, and termination.[15]

(1) Radical generation from non-radical species (initiation)

$$I \xrightarrow{k_d} 2\,R$$

Accordingly, initiators with similar decomposition rates and initiating efficiencies should bring about similar initiation rates irrespective of the monomer.

(2) Radical addition to a substituted alkene (propagation)

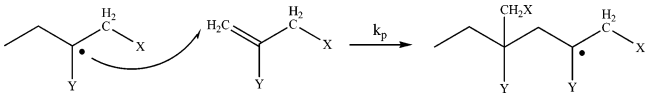

(3) atom transfer (chain transfer) reactions

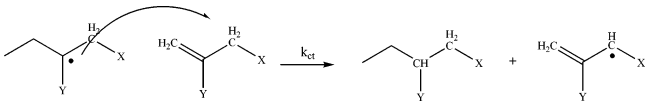

(4) atom abstraction reactions (termination by disproportionation)

and radical−radical recombination reactions (termination by coupling)

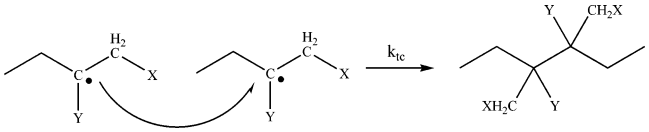

In this study, the radical chain is modeled by a monomer to which a methyl radical is attached as is illustrated in the reaction schemes above.

2. Reaction Kinetics. The reaction rate constants (k_p, k_{ct}, and k_{td}) are calculated by using the conventional transition state theory (TST).[16] Within the transition state theory (TST), the rate constant of a bimolecular reaction A + B → C is related to the molecular properties of the reacting species.[17]

$$k(T) = \frac{k_B T}{h} K_C^{\ddagger}$$

$$K_C^{\ddagger} = \frac{q_{TS}}{q_A q_B} e^{-\Delta E_0/k_B T}$$

where k_B represents Boltzmann's constant, T is the temperature, h is the Planck's constant, ΔE_0 represents the molecular energy difference between the activated complex and the reactants (with inclusion of zero point vibrational energies), and q_{TS}, q_A, and q_B are the molecular partition functions of the transition state and reactants, respectively. The rate constant is expressed per unit volume, per mol, and per unit time. The molecular properties, such as geometries, ground state energies, and frequencies that are required for the evaluation of the partition functions, and the reaction barrier are obtained by ab initio molecular calculations. The kinetic parameters are deduced from fitting the results of the TST expression to the Arrhenius rate law in a specific temperature range. In our case, the temperature range of experimental relevance is 250−350 K. A conformer search analysis has been carried out for all the structures in order to locate the energetically most stable points on the potential energy surface. Intrinsic reaction coordinate (IRC) calculations have been performed to justify the nature of the transition state structures.

The rate of polymerization, R_p, is given by

$$R_p = -\frac{d[M]}{dt} = k_p\left(f\frac{k_d}{k_t}\right)^{0.5}[M][I]^{0.5}$$

where k_p, k_d, and k_t are the rate coefficients corresponding to the propagation, initiator decomposition, and termination steps. f is the initiator efficiency, [M] and [I] are the concentrations of the monomer and initiator, respectively. In this study, the polymerization behavior of monomers whose experimental conditions are more or less similar have been considered. Thus, the parameters related to the initiator, the initiator efficiency f and the rate of the initiator decomposition k_d are taken to be similar under similar experimental conditions.

3. Computational Details. All calculations were carried out with the Gaussian 03 software package.[19] The geometry optimizations are performed at the B3LYP/6-31+G(d) level of theory[20] whereas single point calculations were performed with the new hybrid density functional BMK, which is especially suitable for kinetics and reaction mechanisms.[21] There is a general consensus that B3LYP methods provide excellent low-cost performance for structure optimizations.[22] For energy predictions, however, B3LYP is less accurate and the use of other more advanced functionals with a more reliable performance for reaction energies is desirable. Recent studies have shown that the new hybrid meta-GGA-functional such as BMK (Boese−Martin for kinetics) performs much better with an overall accuracy of a maximum of 8 kJ/mol for the barrier heights.[23] The combination of a high percentage of Hartree−Fock exchange with terms dependent on the kinetic energy density in the functional is the origin of the surprisingly good performance of BMK. BMK can actually be considered as a reliable general-purpose functional whose domain of applicability has been expanded to cover transition states without loosing its accuracy for geometry optimizations. A lot of recent studies confirm these findings.[24] The results are thus obtained with the two-component method BMK/6-311+G(3df,2p)//B3LYP/6-31+G(d). The transition states were verified to have only one imaginary frequency corresponding to the reaction coordinate. It was confirmed by CASSCF(3,6)/6-31+G(d) calculations that the transition states for disproportionation have a single determinant character.

For the construction of the partition functions corresponding to the internal motions of the molecule, a mixed HO/HR approach was adopted. The rotations about the forming or breaking bonds in the transition states were treated using the 1D-HR approach.[25] Several studies have indicated that the account of this specific mode gives the largest corrections to the original HO partition functions, as it allows finding a variety of possible transition states in terms of the rotational angle.[26] All the other internal motions were treated in the standard HO model. The rotational potentials were determined at the B3LYP/6-31+G(d) level of theory, and the modified partition function was determined following the procedure outlined in reference 25.

Results

As outlined in the introduction, the monomers chosen can be classified in three different classes. The monomers in Class I have been chosen in order to assess the effect of the size of pendant groups on the polymerizability of acrylates, those in

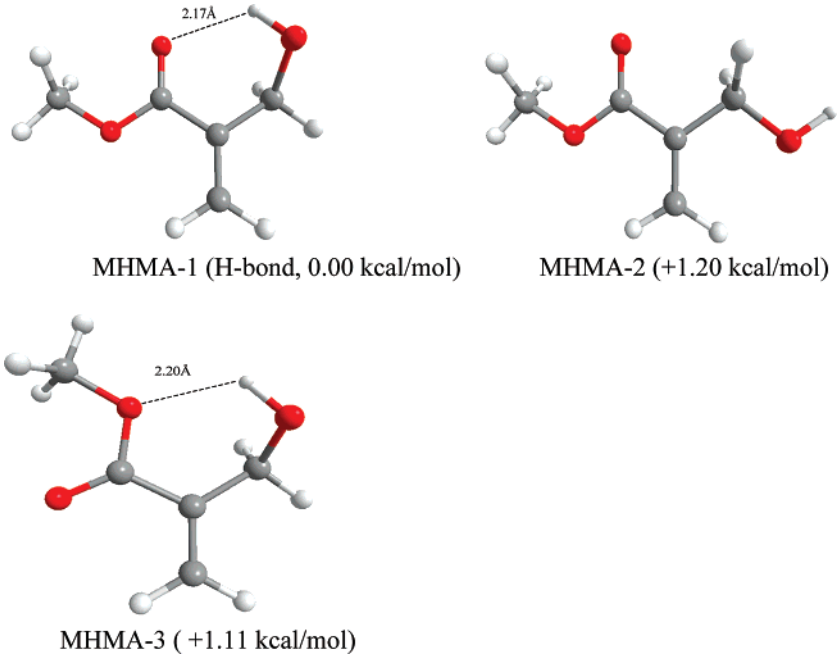

Figure 2. Various conformers of MHMA at the BMK/6-311+G(3df,2p)//B3LYP/6-31+G(d) level.

Class II are expected to enlighten the effect of polarity on the polymerizabilty of acrylates, whereas those in Class III will shed light on the effect of cyclic pendant group on the rate of polymerization of acrylates.

A. Class I: The Effect of Pendant Groups Size on the Polymerizability of Acrylates. Structures of the Monomers. Among the various conformers of MHMA, the structures corresponding to the lowest stationary points on the potential energy surface (PES) are MHMA-1 (0.00 kcal/mol), MHMA-2 (1.20 kcal/mol), and MHMA-3 (1.11 kcal/mol). The relative energies of the structures displayed in Figure 2 include the zero point energies. The internal hydrogen bond between the alcoholic hydrogen and the carbonyl oxygen stabilizes MHMA-1. In MHMA-3, the H-bond is with the carboxyl oxygen rather than the carbonyl oxygen. MHMA-2 is an extended conformation and does not show intramolecular hydrogen bonds.

The structures of the energetically most stable conformers of MHMA, EHMA, and TBHMA are very similar to each other, the H-bond between the alcoholic hydrogen and the carbonyl oxygen is 2.168 Å, to 2.155 Å, and 2.142 Å in MHMA, EHMA and TBHMA, respectively, and stabilizes these species. Notice that in every case, the anti conformer is more stable than the syn due to intramolecular hydrogen bonds. The radicals MHMA-R, EHMA-R, TBHMA-R have a methyl group attached to the olefinic double bond of the monomers ($CH_3-CH_2-C^{\bullet}-(CH_2OH)(CO)-O-R$, where R = CH_3, C_2H_5, C_4H_9). The global minima for these radicals have similar structures as the monomers themselves, they are all stabilized by intramolecular hydrogen bonds between the OH group and the carbonyl oxygen (1.977 Å in MHMA-R, 1.965 Å in EHMA-R, and 1.967 Å in TBHMA-R). The radicalic nature of MHMAR causes an electron delocalization and charge separation ($\delta_O = -0.562$, $\delta_H = 0.506$) as compared to the neutral MHMA ($\delta_O = -0.542$, $\delta_H = 0.492$) and this causes a shortening in the hydrogen bonds.

Influence of Hydrogen Bonding in the Preorganization of the Reactants. We investigated the influence of hydrogen bonding on the reaction kinetics for the propagation reaction of the first monomer, MHMA. Four different transition states (TS1, TS2, TS3, and TS4) have been located, depending on the nature of the hydrogen bonds (see Figure 3). The first transition state TS1 has two intramolecular hydrogen bonds (1.96 and 2.15 Å) whereas the distance of the forming C−C bond (hereafter referred to as the critical distance) is 2.25 Å. A second transition state TS2 has one intermolecular (1.92 Å) and one intramolecular (2.16 Å) H-bond with a critical distance of 2.20 Å. TS3 has two intermolecular bonds (1.93 and 2.00 Å) with a critical distance of 2.30 Å. TS4 has two intramolecular H-bonds (2.18 and 2.00 Å) with a critical distance of 2.25 Å. TS4 (0.00 kcal/mol) is more stable than TS1 (+2.02 kcal/mol), TS2 (+7.51 kcal/mol), and TS3 (+8.05 kcal/mol). IRC calculations starting from the transition state structures have been carried out in order to generate the corresponding reactant complexes. The relative energies of the various reactant complexes and transition states are given in Scheme 1. The complexes corresponding to each transition structure bear the same nomenclature, i.e., RE1 is the reactant complex corresponding to TS1. The reactant complex RE1 with two intermolecular H-bonds (1.89 Å each) is stabilized by 4.33 kcal/mol with respect to the separated reactants. RE2 has one intermolecular (2.26 Å) and one intramolecular H-bond (2.12 Å) and is 2.64 kcal/mol less stable than RE1. RE3 with two intermolecular H-bonds (2.05 Å, 2.04 Å) and RE4 with two intramolecular H-bonds (2.00 and 2.00 Å) are less stable than RE1 by 7.46 and 2.14 kcal/mol, respectively. The stability of RE4 can be attributed to the strength of the hydrogen bonds: 2.00 Å in RE4 as compared to 1.89 Å in RE1. The reactant species in the most stable complex RE1 are not properly organized for the propagation reaction to start. Presumably the intermolecular H-bonds in the most stable complex RE1 loosen, and a reorganization of the reactant molecules takes place allowing the propagation reaction to proceed through the most favorable transition state structure TS4. In Scheme 1, the propagation barrier, E_0, for MHMA starting from the separate reactants is 4.67 kcal/mol.

Avcı et al. have investigated the experimental rates of polymerization of TBHMA as a function of temperature

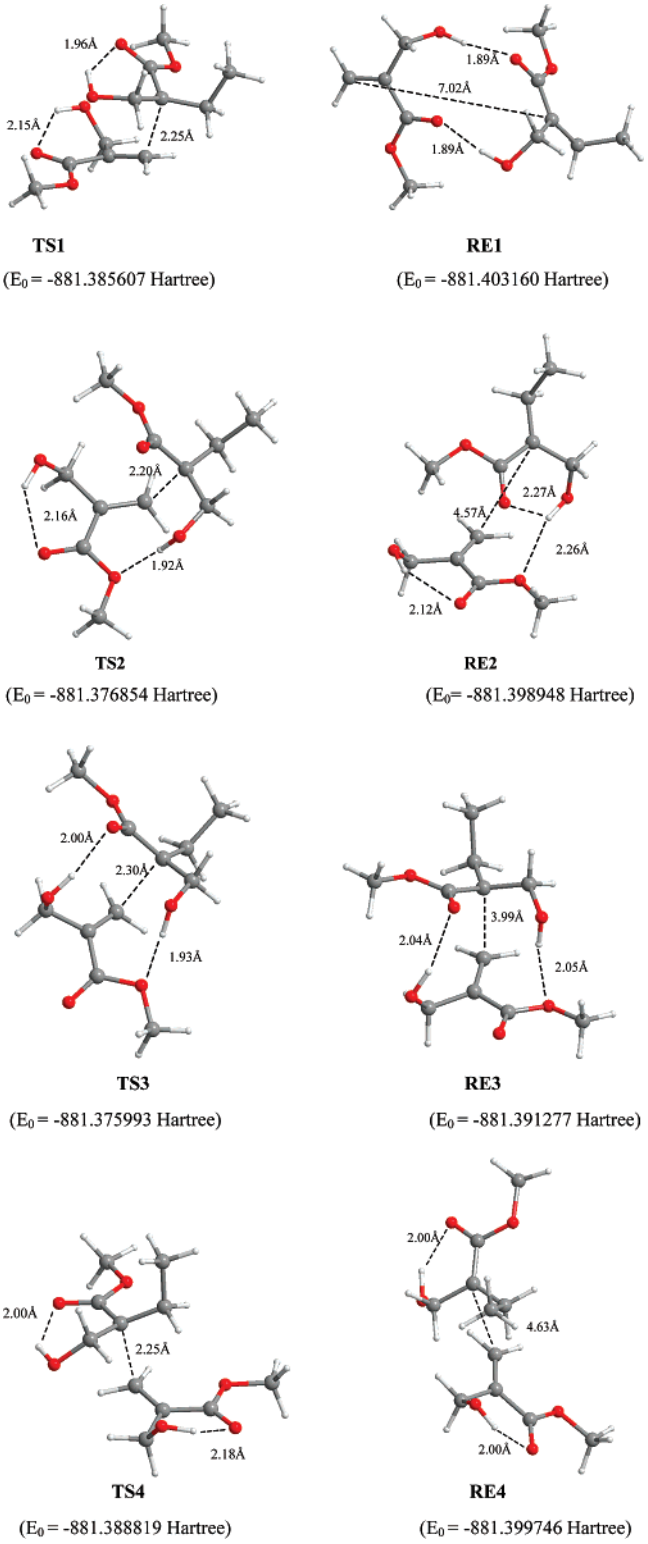

Figure 3. Various transition structures and their corresponding reactant complexes for MHMA (BMK/6-311+G(3df,2p)//B3LYP/6-31+G(d). E_0 is defined as the ground state energy with inclusion of zero point vibrational energy.

(Table 2).[14] Instantaneous rates of polymerization were calculated according to following equation:

$$\text{rate} = \frac{(Q/\text{s})M}{n\Delta H_{\text{theor}} m}$$

where ΔH_{theor} is the heat released per mole of double bonds

Scheme 1. Relative Energies (E_0, kcal/mol) for the Various Transition Structures and Their Corresponding Reactant Complexes for the Propagation Reaction of MHMA (BMK/6-311+G(3df,2p)//B3LYP/6-31+G(d)

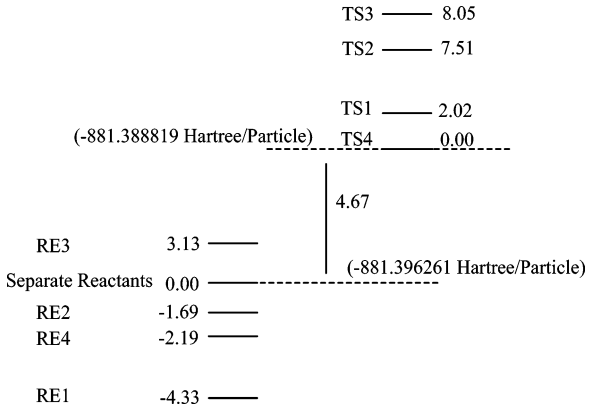

Table 2. Experimental Rates of Polymerization (s^{-1}) and % Conversion for TBHMA

T (°C)	rate	% conversion
35	0.0137	61.9
40	0.0160	69.3
50	0.0161	63.8
65	0.0162	56.1
70	0.0144	46.1

reacted ($\Delta H_{\text{theor}} = 13.1$ kcal/mol for methacrylate double bonds), Q/s is the heat flow per second, M is the molar mass of the monomer, n the number of double bonds per monomer molecule, and m is the mass of the monomer in the sample. Generally, the rate is expected to increase with temperature; however, in this case, due to the presence of intermolecular hydrogen bonding, the rate reaches a limiting value. The fact that the rate of polymerization reaches an almost constant value (0.0160) as the temperature increases, suggests that the heat absorbed is used to destroy the intermolecular H-bonds which might form prior to the polymerization process. Lee et al. report the correlation between the effect of temperature on hydrogen bonding and the effect of temperature on the polymerization rate for the photopolymerization rate of hydroxyalkyl acrylates.[7] They also observe a decrease in the rate of polymerization as a function of time for hydroxyethyl acrylate (HEA) which is found to display intermolecular hydrogen bonds. Our computational results confirm the presence of intermolecular H-bonds in the most stable prereactive complex RE1. In order to proceed with the polymerization, the intermolecular H-bonds in the prereactive complex break down; the radical attacks the monomer through TS4 which is the lowest stable transition state. All plausible transition structures, except for TS3, have intramolecular H-bonds. Thus, even though the monomers preorganize through intermolecular H-bonds, the most favorable intermediate along the propagation reaction is stabilized by intramolecular H-bonds. As claimed by Davis in the study on the propagation reaction in the free radical polymerization of EHMA, complex formation between hydroxy-containing compounds is very probable.[27] De La Rosa et al. have carried out detailed atomistic modeling of the dense glassy isotactic and syndiotactic poly(allyl alcohol) (PAA) and poly(vinyl alcohol)) (PVA). PVA, where six-membered rings between the lateral groups are formed, is stabilized by intramolecular hydrogen bonds.[28] In PAA, the intramolecular hydrogen bonds represent about 60% of the total hydrogen bonds. In the case of PVA where eight-membered rings would form between neighboring groups, intramolecular bonds are of lower occurrence. This study confirms the

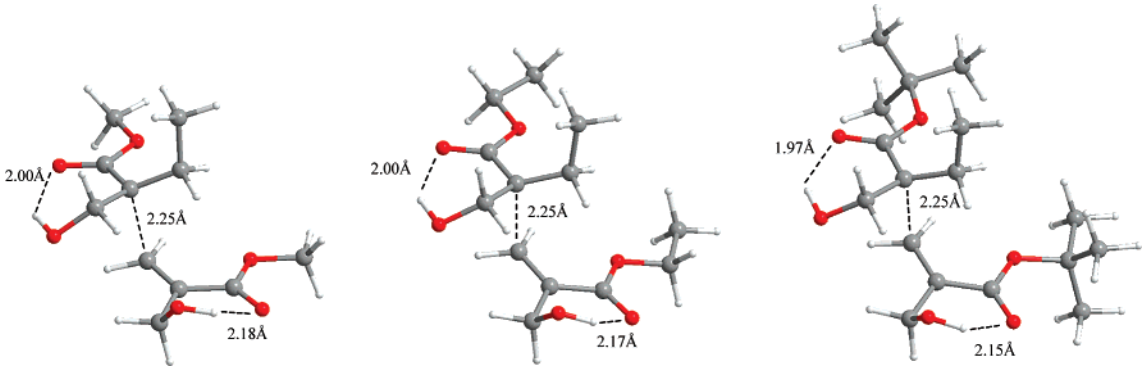

Figure 4. Transition states of the propagation for MHMA, EHMA, and TBHMA (B3LYP/6-31+ G(d)).

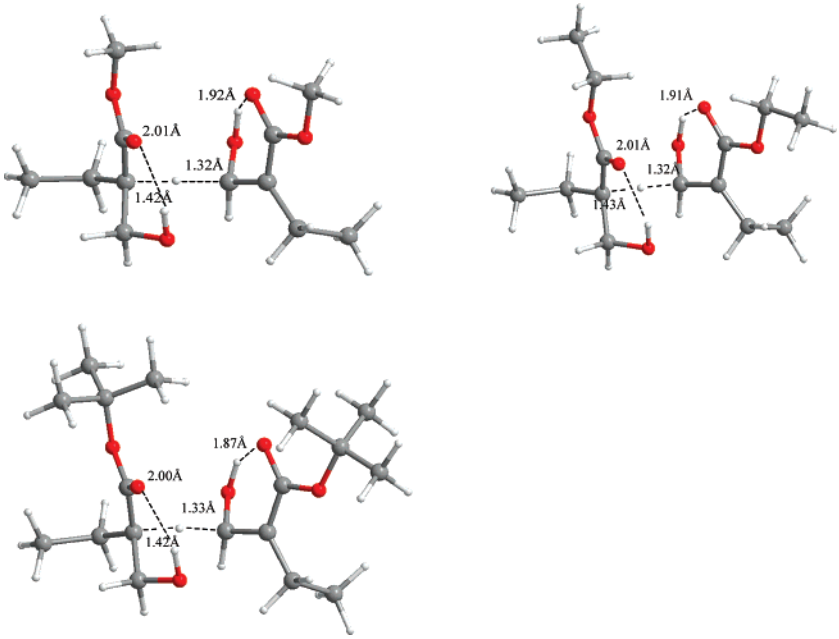

Figure 5. Transition states of the disproportionation reaction of MHMA, EHMA, and TBHMA (B3LYP/6-31+G(d)).

Scheme 2. Mechanism for the Disproportionation Reaction in Class I Monomers

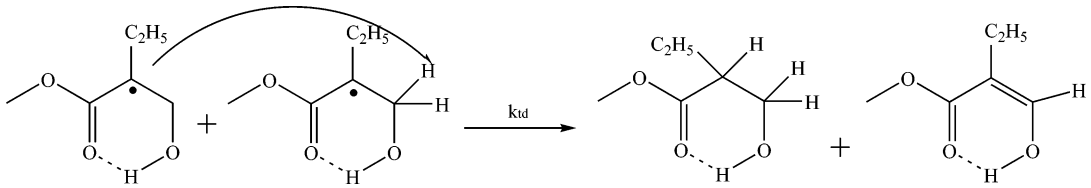

occurrence of intramolecular hydrogen bonds whenever six-membered rings can form as shown above for MHMA.

Reaction Kinetics. The reaction kinetics have been calculated by considering the most stable transition state, TS4 and the separated reactants. The transition states for the propagation reactions corresponding to the other monomers EHMA and TBHMA show a large similarity with each other in the sense that each monomer moiety in the transition state is stabilized by an intramolecular H-bond and a critical distance of about 2.25 Å (Figure 4). However, because of steric hindrance, the propagation reaction for TBHMA is expected to be less facile than the one for MHMA. TBHMA characterized by a bulky isobutyl pendant group has indeed the largest activation energy for propagation, i.e., 6.16 kcal/mol compared to 5.60 kcal/mol for MHMA. The effect of the ester side chain on the propagation kinetics of alkyl methacrylates has been monitored by the pulsed-laser polymerization technique.[30] This study has shown an increase in k_p with ester chain length. In Class I monomers, where the α-substituent is α-hydroxymethyl instead of methyl, the experimentally observed and calculated rates of polymerization decrease with chain length. This behavior can be rationalized by the presence of intramolecular hydrogen bonding which leads to the formation of six-membered rings and prevents the approach of bulky groups.

Experimentally it is known that small, aliphatic radicals terminate predominantly by coupling, and methylmethacrylate undergoes termination both by coupling and disproportionation. The extent of disproportionation in MMA increases from 67% at 25 °C to 80% at 80 °C.[18] It is also known that termination by disproportionation increases when the propagating radical is sterically hindered or has more β-hydrogens available for transfer. For monomers of Class I, there is no experimental evidence for the mode of termination. In this study, we have checked whether disproportionation as shown in Scheme 2 might be the major termination process. The rate constant k_{td} depicts the kinetics of the transfer of hydrogen between two radicals

Table 3. Energetics (kcal/mol) and Rate Coefficents (L mol^{-1} s)[a] for Monomers in Class I (BMK/6-311+G(3df,2p)//B3LYP/6-31+G(d), (250 K < *T* < 350 K)

	propagation reaction				disproportionation reaction			
monomers	A	E_a	ΔH	k_p	E_a	k_{td}	k_p(rel)	R_{expt}(rel)
MHMA	1.46×10^2	5.60	−18.2	1.62×10^{-2}	16.15	1.59×10^{-9}	1.00	1.00
EHMA	7.49×10^1	5.96	−17.7	4.75×10^{-3}	16.55	3.52×10^{-10}	0.29	0.81
TBHMA	1.27×10^2	6.16	−17.3	4.52×10^{-3}	17.73	4.85×10^{-11}	0.28	0.43

[a] Rate coefficients calculated at 300 K, were corrected by using the HR correction factors of 1.33 for MHMA, 1.39 for EHMA, and 1.10 for TBHMA in the propagation and by 1.74 for MHMA, 1.61 for EHMA, and 1.92 for TBHMA in the disproportionation reactions, respectively. These factors are included in the calculations.

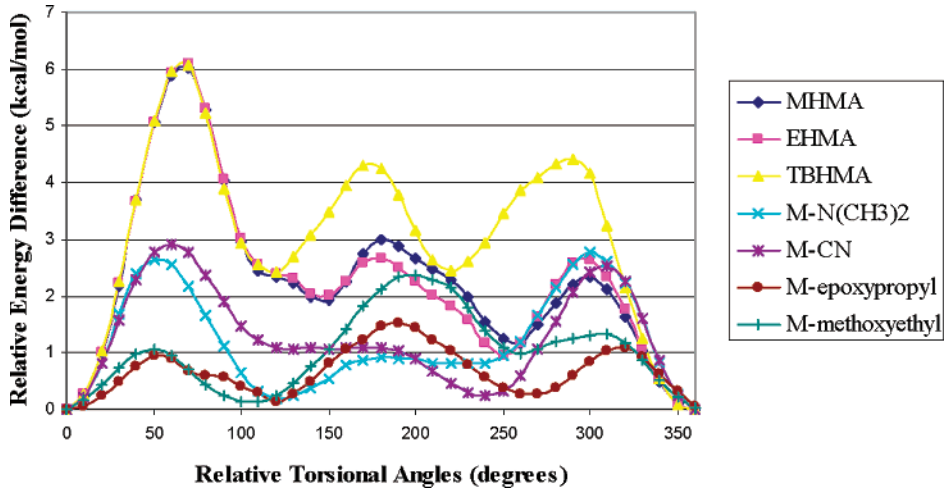

Figure 6. Rotational potentials (B3LYP/6-31+G(d)) for the propagation reactions.

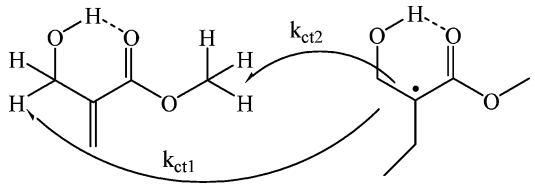

Figure 7. Mechanism for the chain transfer reaction for MHMA in Class I monomers.

(Figure 5). The termination by coupling has not been modeled, as these reactions where two radicals couple need advanced and very expensive molecular modeling techniques which are beyond the scope of this study. The accurate a priori prediction of the high-pressure rate coefficient for radical−radical combination reactions has been a difficult challenge since the location of the reaction bottleneck shifts dramatically as a function of the energy and the angular momentum of the collision.[31] Recently, an ab initio transition state theory based procedure at the CASPT2/cc-pvdz level within the variable reaction coordinate-transition state theory (VRC-TST) for accurately predicting the combination kinetics of two alkyl radicals has been reported by Klippenstein et al.[32] However, these methodologies need to be tested for radicals involving unsaturated and resonantly stabilized radicals like the ones in this study.

The activation barriers for the disproportionation reactions are higher than the ones for the propagation reactions as expected (Table 3). The values of k_p reproduce the desired trend, in that steric hindrance inhibits the rate of propagation: i.e., k_p(MHMA) > k_p(EHMA) > k_p(TBHMA). As is evidenced by the magnitude of k_{td}, the disproportionation reaction is quite slow and is probably not the rate-determining step for the termination process of monomers of Class I. Considering the ratio $k_p/k_{td}^{1/2}$ as an indicator of the polymerizability trend overestimates the importance of disproportionation within the termination process. Overall, the relative experimental trend in polymerizability for monomers of Class I is relatively well reproduced with the relative propagation rate constants k_p. As indicated in the last two columns of Table 3, from the reaction rates of disproportionation it might be that coupling would be important for termination.

Influence of Internal Rotation About the Forming Bond on the Reaction Kinetics. The rotation about the forming bond in the transition state has been modeled using the 1D-HR approach as introduced in ref 25. MHMA and EHMA show very similar rotational profiles: two additional minima come into play but they all lie higher in energy than the reference conformer. Moreover a substantial energy barrier is needed to reach the other transition states, due to large steric hindrance between the bulky subsituents of the radical and the monomer. For TBHMA, the potential is characterized by higher rotational barriers due to the presence of additional bulky groups which prevent rotation in the transition state. Rotational potentials for the propagation reaction of monomers are displayed in Figure 6. The correction factors are 1.33 (1.74), 1.39 (1.61), and 1.10 (1.92) for the propagation (disproportionation) reactions of MHMA, EHMA, and TBHMA, respectively. The correction factors by applying the 1D-HR approach all lie close to 1, as all additional transition states that come into play lie substantially higher in energy than the reference conformer.

How Important is the Chain Transfer to the Monomer for Class I Monomers? An important class of reactions that can influence the normal propagation is the chain transfer to monomer in which the radical is transferred to the monomer by hydrogen abstraction or hydrogen transfer. The rate constant for chain transfer to monomer is referred to as k_{ct}. Thereby a small radical species is generated originating from the former monomer which can reinitiate by attacking a second monomer. The rate constant for reinitiation is called k_a.

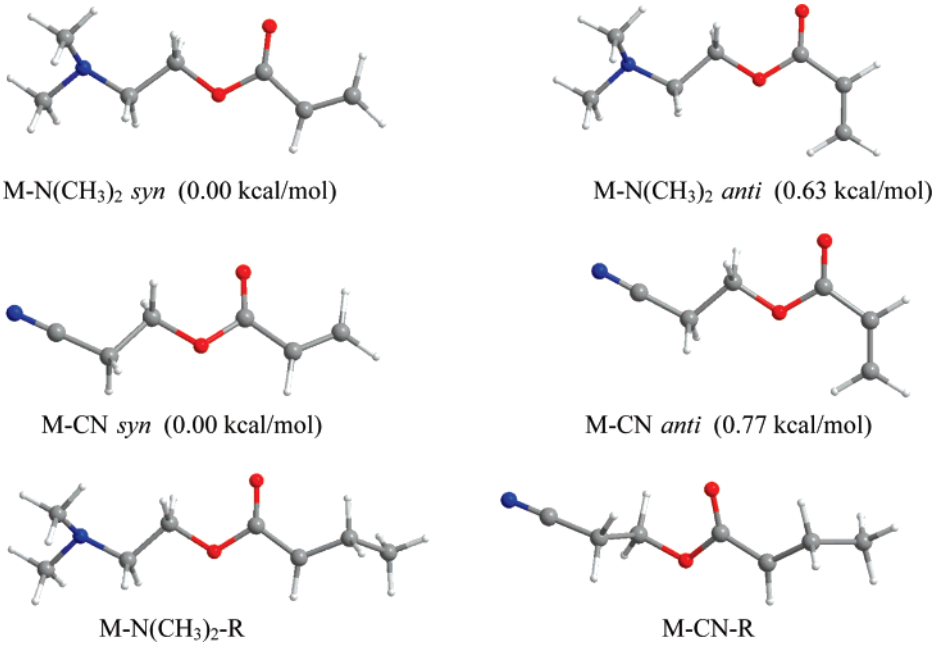

Figure 8. Most stable syn and anti conformers of M−$N(CH_3)_2$, M−CN, M−$N(CH_3)_2$−R, and M−CN−R calculated at the B3LYP/6-31+G(d) level of theory.

Table 4. Energetics (kcal/mol) and Rate Coefficients (L mol^{-1} s) for Chain Transfer for Monomers in Class I (BMK/6-311+G(3df,2p)//B3LYP/6-31+G(d), (250 K < *T* < 350K)

monomers		A	E_a	k_{ct1}	k_{ct2}	k_p
MHMA	R-hydrogen	3.62×10^3	21.88		1.26×10^{-12}	1.62×10^{-2}
	α-hydrogen	2.76×10^3	13.76	5.19×10^{-7}		
EHMA	R-hydrogen	2.63×10^7	26.24		1.00×10^{-11}	4.75×10^{-3}
	α-hydrogen	1.63×10^3	13.95	2.25×10^{-7}		
TBHMA	R-hydrogen	2.65×10^3	25.35		8.15×10^{-15}	4.52×10^{-3}
	α-hydrogen	7.57×10^2	14.05	8.97×10^{-8}		

Table 5. Propagation Rate Constant (k_p) for EHMA (250 K < *T* < 350 K)[a]

solvent	ϵ	B3PW91/ 6-31+G(d)	MPW1K/ 6-31+G(d)	MPW1PW91/ 6-31+G(d)	B3LYP/ 6-31+G(d)	BMK/ 6-31+G(d)	exptl[27] k_p
gas[b]		1.01×10^{-4}	1.34×10^{-3}	1.97×10^{-3}		4.75×10^{-3}	
toluene	2.3	5.13×10^{-6}	6.42×10^{-5}	9.60×10^{-5}	1.46×10^{-6}	3.95×10^{-4}	1600
chloroform	4.8	4.25×10^{-7}	4.38×10^{-6}	7.62×10^{-6}	1.26×10^{-7}	2.82×10^{-5}	909
ethanol	24.3	5.63×10^{-8}	4.92×10^{-7}	9.73×10^{-7}	1.73×10^{-8}	3.29×10^{-6}	589

[a] All the structures have been optimized at the B3LYP/6-31+G(d) level. [b] Energetics in the gas phase are at the 6-311+G(3df,2p) level.

Scheme 3. Mechanism for the Disproportionation Reaction in Class II and Class III

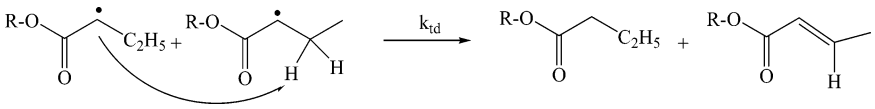

During a free radical polymerization reaction, the radical R• can either propagate by attacking the monomer with the rate constant k_p(propagation reaction)

$$M + R^{\bullet} \xrightarrow{k_p} M{-}R^{\bullet}$$

or abstracting a hydrogen from the monomer with the rate constant k_{ct} (chain-transfer reaction)

$$M + R^{\bullet} \xrightarrow{k_{ct}} R{-}H + (M{-}H)^{\bullet}$$

Chain transfer yields a saturated compound (R−H) and a new radical whose hydrogen has been abstracted $(M-H)^{\bullet}$ (Figure 7). The results in Table 4 show that chain transfer in unimportant for this class of monomers.

$$(M{-}H)^{\bullet} + M \xrightarrow{k_a} \text{polymer}$$

Benchmark Calculations on Solvent and Level of Theory (LOT) Study on the Propagation Reaction of EHMA. Benchmark calculations have been carried out for EHMA since experimental results[27] were already present in the literature. All the functionals reproduce the experimental trend qualitatively in that the propagation rate constant decreases in polar medium. The effect of a polar environment was taken into account by use of the self-consistent reaction field (SCRF) theory, utilizing the integral equation formalism-polarizable continuum[33] (IEF-PCM) model in solution. Notice that even though special interactions with the solvent (H-bonding) are not taken into account, the experimental trend is quite well reproduced with geometries taken from B3LYP/6-31+G(d) with all functionals and even slightly better with BMK (Table 5).

Table 6. Energetics (kcal/mol), and Rate Coefficients (L mol^{-1} s)[a] for Monomers in Class II (BMK/6-311+G(3df,2p)//B3LYP/6-31+G(d)) (250 K < *T* < 350 K)

	propagation reaction			kinetics			
monomers	A	E_a	ΔH	k_p	k_{td}	$k_{p(rel)}$	R_{expt}(rel)
M−N(CH$_3$)$_2$	1.86×10^2	6.74	−19.97	7.05×10^{-3}	2.98×10^{-12}	1.00	1.00
M−CN	3.06×10^2	6.78	−19.70	9.57×10^{-3}	2.12×10^{-12}	1.36	12.60

[a] Rate coefficients for propagation were corrected by using the HIR correction factors of 3.33 for M−N(CH$_3$)$_2$ and 2.91 for M−CN.

Table 7. Reinitiation Rate Constants for M−N(CH$_3$)$_2$, M−CN (BMK/6-311+G(3df,2p)//B3LYP/6-31+G(d)), (250 K < T < 350 K)

monomer	k_{ct1}	k_{ct2}	k_{ct3}	$k^*_{ct\ (total)}$	k_a	k_p	k_a'
(A) Reinitiation Rate Constants[a]							
M−N(CH$_3$)$_2$	2.24×10^{-6}	1.15×10^{-6}	4.45×10^{-10}	1.14×10^{-5}	8.88×10^{-1}	7.05×10^{-3}	1.43×10^{-3}
M−CN	4.93×10^{-9}	5.44×10^{-10}		1.09×10^{-8}	2.50×10^{-3}	9.57×10^{-3}	2.86×10^{-9}
(B) Reinitiation Rate Constants with Eckart Tunneling and Free Rotor Corrections							
M−N(CH$_3$)$_2$	4.67×10^{-5}	2.08×10^{-5}	4.45×10^{-10}	2.18×10^{-4}	8.88×10^{-1}	7.05×10^{-3}	2.75×10^{-2}
M−CN	3.01×10^{-7}	5.44×10^{-10}		6.03×10^{-7}	2.50×10^{-3}	9.57×10^{-3}	1.58×10^{-7}
(C) Reinitiation Rate Constants with Wigner Tunneling and Free Rotor Corrections[b]							
M−N(CH$_3$)$_2$	7.08×10^{-6}	3.53×10^{-6}	4.45×10^{-10}	3.53×10^{-5}	8.88×10^{-1}	7.05×10^{-3}	4.45×10^{-3}
M−CN	1.81×10^{-8}	5.44×10^{-10}		3.74×10^{-8}	2.50×10^{-3}	9.57×10^{-3}	9.77×10^{-9}

[a] For M−N(CH$_3$)$_2$, $k_{ct\ (total)} = 2k_{ct1} + 6k_{ct2} + 2k_{ct3}$; for M−CN, $k_{ct\ (total)} = 2k_{ct1} + 2k_{ct2}$. Rate coefficients were corrected by using the free rotor correction factors for M−N(CH$_3$)$_2$ (5.0, 4.6, and 8.5 for k_{ct1}, k_{ct2}, and k_{ct3}) and for M−CN (7.1, 7.3 for k_{ct1}, k_{ct2}). [b] For M−N(CH$_3$)$_2$, $k_{ct\ (total)} = 3.16(2k_{ct1}) + 3.07(6k_{ct2}) + 2k_{ct3}$. For M−CN, $k_{ct\ (total)} = 3.68(2\ k_{ct1}) + 2k_{ct2}$.

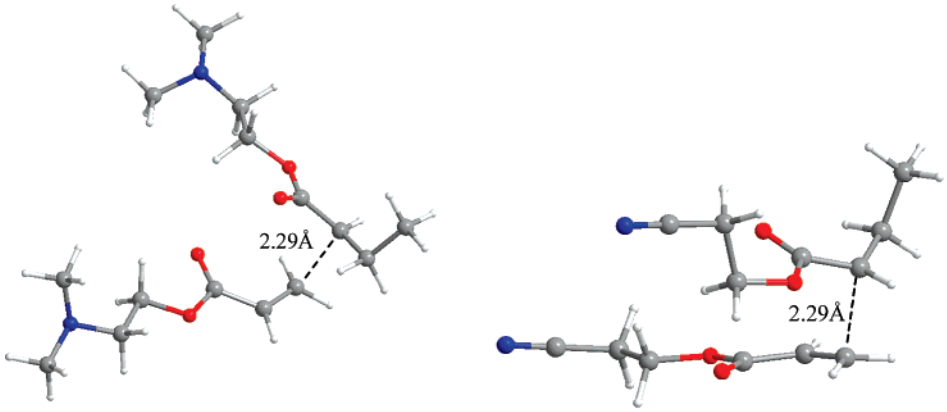

Figure 9. Transition states of propagation for M−N(CH$_3$)$_2$ and M−CN (B3LYP/6-31+G(d)).

B. Class II: Effect of Polar Groups on the Polymerizability of Acrylates. Structures of the Monomers. The syn and anti conformations for M−N(CH$_3$)$_2$ and M−CN have been modeled, and the ones lowest in energy (E_0) are displayed in Figure 8. For both monomers, the syn conformations have been found to be more stable at the B3LYP/6-31+ G(d) level. The structures corresponding to the global minima for the monomers and the radicals are quite extended, minimizing the unfavorable steric interactions and maximizing the favorable bifurcated C═O···H interactions.

Reaction Kinetics. The transition states for propagation of monomers M−N(CH$_3$)$_2$ and M−CN are shown in Figure 9. The distance of the forming bond for the transition states of Class II is slightly larger than for monomers of Class I (2.29 versus 2.25 Å). It can be anticipated that the activation energy for Class II monomers will be higher, as for addition reactions to double bonds, a correlation exists between the critical distance and the activation energy. For more information, we refer to the review paper by Fisher and Radom.[29] We have checked whether termination is dominated by disproportionation (as shown in Scheme 3).

In this case the barriers for rotation are significantly lower than for Class I monomers, due to considerably less steric hindrance between substituents of the monomer and the radical. The double bond of the olefin is now unsubstituted at one end, explaining the easier rotation about the forming bond. Additional minima along the rotational potential have nearly the same energy as the reference conformer. Consequently, the correction factors for propagation are larger than for Class I monomers, i.e., 3.33 and 2.91 for M−N(CH$_3$)$_2$ and M−CN, respectively. These factors obtained by applying the 1D-HR approach are non-negligible and might be important for a correct reproduction of the polymerization trend.

The activation barrier for propagation of Class II monomers is slightly higher than the one for Class I monomers, whereas the pre-exponential factors show more subtle variations with respect to Class I (as shown in Table 6). M−CN is smaller and more compact than M−N(CH$_3$)$_2$ and its pre-exponential factor is larger than the one for M−N(CH$_3$)$_2$, thus $\Delta S^{\ddagger}$ is larger for the former. The entropy of activation, $\Delta S^{\ddagger}$ renders k_p larger in the case of M−CN even though the activation barriers for the propagation reaction are more or less similar. As in Class I, for monomers of Class II the disproportionation pathway is not rate determining in terms of termination. The trend in k_p (1.4:1) mimics qualitatively the experimental trend (14:1); however, consideration of the propagation rate constant only underestimates the polymerization trend on a quantitative basis. To understand the discrepancy further, the role of side reactions for these monomers has been investigated by modeling the chain transfer reactions.

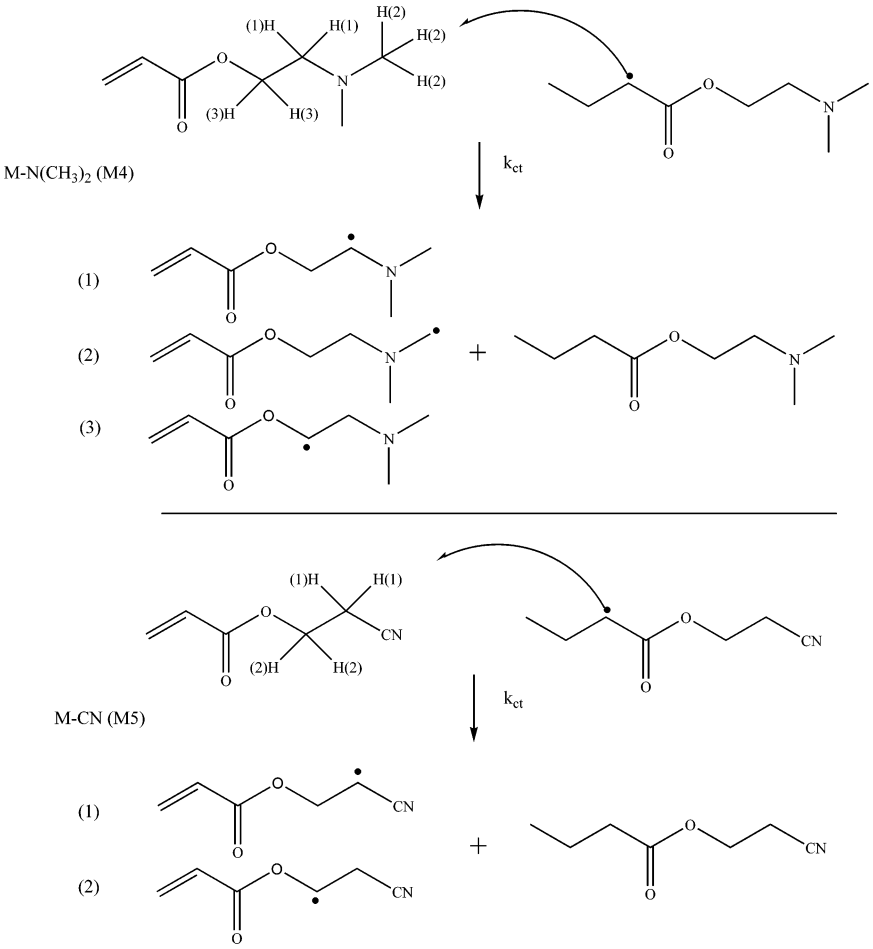

Figure 10. Schematic representation of the chain transfer reactions for monomers M−N(CH$_3$)$_2$ and M−CN.

How Important Is the Chain Transfer to the Monomer for Class II Monomers? As displayed in Table 7, the chain transfer rate constant k_{ct1} is the one for the abstraction of the most labile hydrogens, those on the carbon atom bearing the −N(CH$_3$)$_2$ and CN groups, k_{ct2} is the chain transfer rate constant for abstraction of hydrogens from the N(CH$_3$)$_2$ group in M−N(CH$_3$)$_2$ and from the −CH$_2$−(O)− group in M−CN, k_{ct3} is the chain transfer rate constant for abstraction of hydrogens from the −CH$_2$−(O)− group in M−N(CH$_3$)$_2$. The overall chain transfer constant $k_{ct\,(total)}$ for M− N(CH$_3$)$_2$ (1.14×10^{-5}) is much larger than the transfer rate constant for M−CN (1.09×10^{-8}) indicating that the polymerization in the case of M− N(CH$_3$)$_2$ is inhibited by chain transfer. Schematic representation of the chain transfer reactions for Class II monomers are given in Figure 10.

Furthermore, with dependence on the magnitude of the chain transfer rate constant k_{ct}, reinitiation can compete with propagation. Comparison of k_p and k_a requires normalization of k_a by the normalization factor k_{ct}/k_p. Therefore a modified rate constant k_a' ($k_a' = k_a(k_{ct}/k_p)$) has been introduced.

If $k_{ct} \ll k_p$, then the effect of chain transfer on the reaction is determined by comparing k_a' with k_p.[1] The results in Table 7 demonstrate that reinitiation is unimportant for M−CN for which $k_a' \ll k_p$. However, for M−N(CH$_3$)$_2$, reinitiation can compete with the propagation reaction and this is expected to decrease the polymerizability of the latter.

Tunneling corrections have been introduced with Eckart[34] and Wigner[35] methodologies in order to test the effect of tunneling on chain transfer via hydrogen abstraction. Parts B and C in Table 7 mimic the same qualitative trend as the results in Part A. The value of k_a' with both methods emphasizes further the importance of reinitiation for M−N(CH$_3$)$_2$.

Table 8. Mulliken Charges on Monomers and Radicals of Class II (B3LYP/6-31+G(d))

Compounds	Mulliken charges
M-N(CH$_3$)$_2$	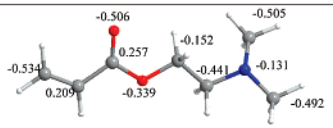
M-N(CH$_3$)$_2$-R	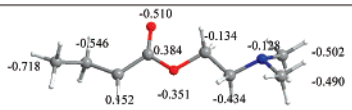
M-CN	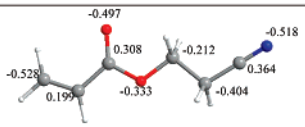
M-CN-R	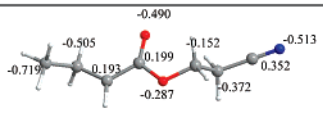

Overall, for monomers in Class II where the nature of the substituents is completely different, i.e., N(CH$_3$)$_2$ vs CN, modeling side reactions such as chain transfer and reinitiation is quite important. Even though the propagation rate constants reproduce the experimental behavior of these monomers qualitatively, the role of chain transfer must be emphasized

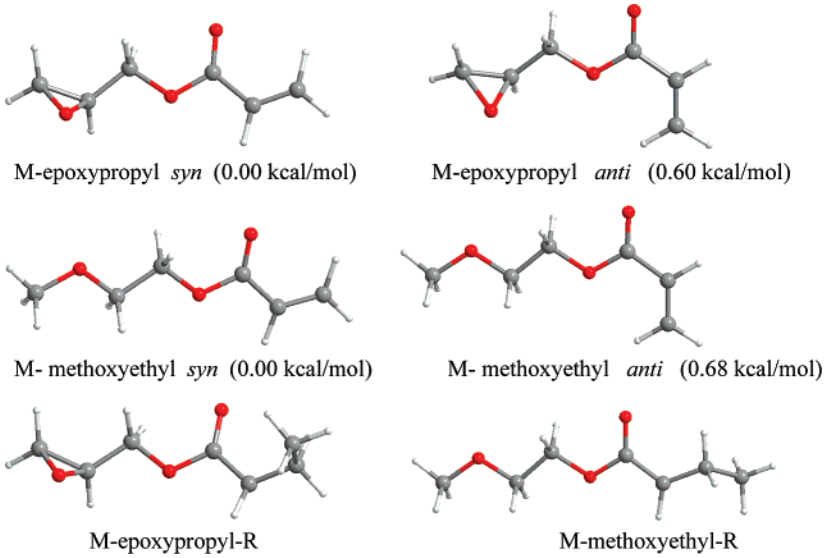

Figure 11. 3D structures for M−epoxypropyl, M−epoxypropyl−R, M−methoxypropyl, and M−methoxyethyl−R (B3LYP/6-31+G(d)).

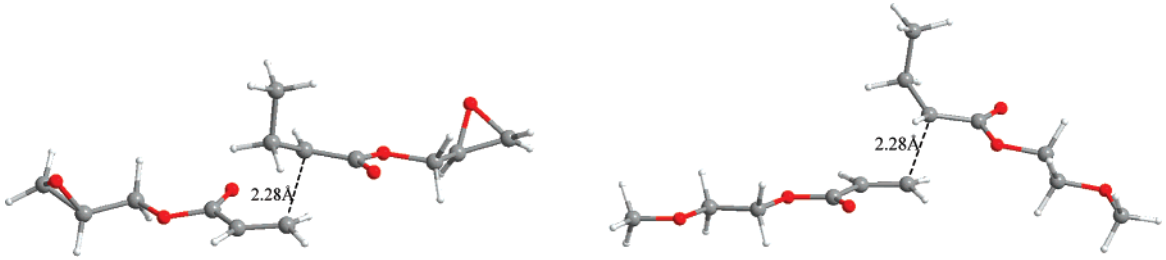

Figure 12. Transition states of the propagation reactions for M−epoxypropyl and M−methoxyethyl (B3LYP/6-31+G(d)).

Table 9. Energetics (kcal/mol) and Rate Coefficients (L mol^{-1} s)[a] for Monomers in Class III (BMK/6-311+G(3df,2p)//B3LYP/6-31+G(d), (250 K < *T* < 350 K)

	propagation reaction			kinetics			
monomers	A	E_a	ΔH	k_p	k_{td}	$k_{p(rel)}$	R_{expt}(rel)
M−epoxypropyl	1.45×10^3	6.95	−20.36	3.72×10^{-2}	2.71×10^{-11}	1.20	1.54
M−methoxyethyl	2.27×10^3	7.10	−20.26	3.11×10^{-2}	1.05×10^{-11}	1.00	1.00

[a] Rate coefficients were corrected by using the HIR correction factors of 3.22 for M−epoxypropyl and 2.21 for M−methoxyethyl.

in understanding the experimental behavior of these monomers.

Charge Distributions and Dipole Moments. On the basis of AM1 calculations, Jansen has attributed the outstanding polymerizability of M−CN to its higher dipole moment (3.7 D) in comparison to the one of M−N(CH$_3$)$_2$ (2.01 D).[3] We have calculated (B3LYP/6-31+G(d)) the dipole moment of both M−N(CH$_3$)$_2$ and M−CN as described by Jansen by averaging it over five conformers. Our findings are such that M−CN has a higher average dipole moment $\langle\mu\rangle$, (4.65 D) as compared to the one of M−N(CH$_3$)$_2$ (2.38 D). Because of their high dipole moments, M−CN molecules are expected to be well organized and facilitate the polymerization.

$$\langle\mu\rangle = \sum_j D_j \frac{e^{-\Delta H_j/RT}}{\sum_j e^{-\Delta H_j/RT}}$$

The Mulliken charge distributions in M−N(CH$_3$)$_2$−R, M−N(CH$_3$)$_2$R, M−CN, and M−CN−R have been used to predict the electrostatic interactions between the radical center and the unsaturated C (Table 8). The electrostatic force of attraction is 0.019 ((−0.528)(0.193)/(2.29)^2) in the case of M−CN and its radical; it is 0.015 ((−0.534)(0.152)/(2.29)^2) in the case of M−N(CH$_3$)$_2$ and its radical. This finding further supports the fact that the polymerization is more facile in the case of M−CN. Overall, the dipole moments and Mulliken charge distributions complement the data generated for the kinetics of these two monomers.

C. Class III: Effect of Cyclic Pendant Groups in Acrylates. Structures of the Monomers. The structures corresponding to global minima for the monomers and the radicals are in the syn conformation, quite extended and similar to each other (Figure 11).

The transition states for propagation are shown in Figure 12. The structures of the transition states of the propagation reactions for M−epoxypropyl and M−methoxyethyl are different than for Class II monomers (dihedrals about forming bonds ∼−60°, 90°) as the pendant groups are situated on the opposite side of the forming bond (dihedrals about forming bonds ∼180°, 90°). The rotational potentials about the forming bond are shown in Figure 6.

Reaction Kinetics. The propagation reaction is favored for M−epoxypropyl. The activation energy for propagation and disproportionation for monomers of Class III are slightly higher

than the values found for monomers of Classes I and II (as shown in Table 9). The trend in k_p values (1.2:1) mimics almost quantitatively the experimental trend (1.5:1). Notice that the rate constant for the disproportionation reaction k_{td} is very small as in the other cases and cannot be considered as the rate determining step for termination.

Conclusion

In this study, polymerization trends within three classes of acrylates/methacrylates were modeled by density functional based methods. Experimentally it was found that the effect of pendant group size, the polarity of the pendant group, and the nature of a cyclic pendant group can influence the polymerization rate substantially. The rates for propagation were calculated using the transition state theory in the relevant temperature range using the two component BMK/6-311+G(3df,2p)//B3LYP/6-31+G(d) level of theory. Moroever the hindered rotor approach was applied for rotation of the monomer and radical about the forming bond. For Class I, the effect of additional transition states by rotating about the forming bond is very small, as they are substantially higher in energy and the rotational barriers are relatively large. For Class II and Class III monomers, the effect is non-negligible with correction factors of about three.

Overall within the present approach, the polymerization trends are qualitatively well reproduced with k_p within each class. However, within Class II when the polar groups exibit large structural differences, the chain transfer to monomer can contribute largely in inhibiting the polymerization. For all monomers it was investigated whether disproportionation would be the major route for termination. This seems to not be the case, most probably coupling will be important.

Acknowledgment. The computational resources used in this work were provided by the TUBITAK ULAKBIM High Performance Computing Center, the Bogazici University Research Foundation (Projects 03M501 and 05HB501), Tubitak (Project 105T223), and the Center of Molecular Modeling, University of Ghent. K.V.C., V.V.S., and M.W. acknowledge the Fund for Scientific Research Flanders (FWO) and the Fund for Scientific Research of the Ghent University for their financial support. The authors acknowledge the sixth framework project COSBIOM (Project FP6-2004-ACC-SSA-2,517991) for funding the travel and lodging expenses of I.D. and V.V.S. in University of Ghent and Bogazici University.

References and Notes

(1) Odian, G. *Principles of Polymerization*; Wiley-Interscience, New York, 1991.

(2) (a) Izgorodina, E. I.; Coote, M. L. *Chem. Phys.* **2006**, *324*, 96−110. (b) Huang, D. M.; Monteiro, M. J.; Gilbert, R. G. *Macromolecules* **1998**, *31*, 5175−5187. (c) Van Speybroeck, V.; Van Cauter, K.; Coussens, B.; Waroquier, M. *ChemPhysChem* **2005**, *6*, 180−189.

(3) (a) Jansen, J. F. G. A.; Dias, A. A.; Dorschu, M.; Coussens, B. *Macromolecules* **2003**, *36*, 3861−3873. (b) Jansen, J. F. G. A.; Dias, A. A.; Dorschu, M.; Coussens, B. *Macromolecules* **2002**, *35*, 7529−7531.

(4) (a) Decker, C.; Moussa, K. *Macromolecules* **1989**, *22*, 4455−4462. (b) Decker, C.; Moussa, K. *Makromol. Chem.* **1991**, *192*, 507−522. (c) Moussa, K.; Decker, C. *J. Polym. Sci., Part A: Polym. Chem.* **1993**, *31*, 2197−2203. (d) Decker, C.; Moussa, K. *Makromol. Chem., Rapid Commun.* **1990**, *11*, 159. (e) Decker, C.; Moussa, K. *Eur. Polym. J.* **1991**, *27*, 881−889.

(5) Decker, C.; Moussa, K. *Polym. Mater. Sci. Eng.* **1989**, *60*, 547.

(6) Andrzejewska, E.; Andrzejewski, M. *J. Polym. Sci., Part A: Polym. Chem.* **1998**, *36*, 665−678.

(7) Lee, T. Y.; Roper, T. M.; Jönsson, E. S.; Guymon, C. A.; Hoyle, C. E. *Macromolecules* **2004**, *37*, 3659−3665.

(8) Beckel, E. R.; Nie, J.; Stansbury, J. W.; Bowman, C. N. *Macromolecules* **2004**, *37*, 4062−4069.

(9) (a) Ueda, M.; Ishibashi, S.; Suzuki, T.; Masuko, T.; Pittman, C. U. *J Polym Sci., Part A: Polym. Chem. Ed.* **1984**, *22*, 2305−2316. (b) Ueda, M.; Yazawa, M.; Suzuki, T.; Pittman, C. U. *J Polym Sci., Part A: Polym. Chem. Ed.* **1986**, *24*, 3177−3189. (c) Ueda, M.; Koyama, T.; Mano, M.; Yazawa, M. *J. Polym. Sci., Part A: Polym. Chem. Ed.* **1989**, *27*, 751−762.

(10) (a) Gunaydin, H.; Salman, S.; Tuzun, N. S.; Avcı, D.; Aviyente, V. *Int. J. Quantum Chem.* **2005**, *103*, 176−189. (b) Salman, S.; Ziylan Albayrak, A.; Avcı, D.; Aviyente, V. *J. Polym. Sci., Part A: Polym. Chem.* **2005**, *43*, 2574-2583.

(11) Lalevee, J.; Allonas, X.; Fouassier, J. P. *J. Phys. Chem. A* **2004**, *108*, 4326−4334.

(12) Avcı, D.; Mathias, L. J.; Thigpen, K. *J. Polym. Sci., Part A: Polym. Chem.* **1996**, *34* (15), 3191−3201.

(13) Smith, T. J.; Shemper, B. S.; Nobles, J. S.; Casanova, A. M.; Ott, C.; Mathias, L. J. *Polymer* **2003**, *44*, 6211−6216.

(14) Avcı, D. Private communications, 2006.

(15) *Handbook of Radical Polymerization*; Matyjaszewski, K, Davis, T. P., Eds.; Wiley-Interscience, A John Wiley and Sons, Inc. Publication: Hoboken, NJ, 2002.

(16) (a) Laidler, K. J.; Hase, W. L.; Hynes, J. T. *J. Phys. Chem.* **1983**, *87*, 2664−2682. (b) Laidler, K. J.; King, M. C. *J. Phys. Chem.* **1983**, *87*, 2657−2664. (c) Pechukas, P. *Annu. Rev. Phys. Chem.* **1981**, *32*, 159−177. (d) Pechukas, P. *Ber. Bunsen-Ges. Phys. Chem.* **1982**, *86*, 372. (e) Truhlar, D.; Garrett, B. C.; Klippenstein, S. J. *J. Phys. Chem.* **1996**, *100*, 12771−12800.

(17) McQuarrie, D. A.; Simon, J. D. *Physical Chemistry: A Molecular Approach*; University Science Books: Sausalito, CA,1997.

(18) (a) Bonta, G.; Gallo, B. M.; Russo, S.; Uliana, C. *Polymer* **1976**, *17*, 217−220. (b) Ayrey, G.; Humphrey, M. J.; Poller, R. C. *Polymer* **1977**, *18*, 840−844. (c) Bamford, C. H.; Eastmond, G. C.; Whittle, D. *Polymer* **1969**, *10*, 771−783.

(19) Frisch, M. J.; Trucks, G. W.; Schlegel, H. B.; Scuseria, G. E.; Robb, M. A.; Cheeseman, J. R.; Montgomery, J. A., Jr.; Vreven, T.; Kudin, K. N.; Burant, J. C.; Millam, J. M.; Iyengar, S. S.; Tomasi, J.; Barone, V.; Mennucci, B.; Cossi, M.; Scalmani, G.; Rega, N.; Petersson, G. A.; Nakatsuji, H.; Hada, M.; Ehara, M.; Toyota, K.; Fukuda, R.; Hasegawa, J.; Ishida, M.; Nakajima, T.; Honda, Y.; Kitao, O.; Nakai, H.; Klene, M.; Li, X.; Knox, J. E.; Hratchian, H. P.; Cross, J. B.; Bakken, V.; Adamo, C.; Jaramillo, J.; Gomperts, R.; Stratmann, R. E.; Yazyev, O.; Austin, A. J.; Cammi, R.; Pomelli, C.; Ochterski, J. W.; Ayala, P. Y.; Morokuma, K.; Voth, G. A.; Salvador, P.; Dannenberg, J. J.; Zakrzewski, V. G.; Dapprich, S.; Daniels, A. D.; Strain, M. C.; Farkas, O.; Malick, D. K.; Rabuck, A. D.; Raghavachari, K.; Foresman, J. B.; Ortiz, J. V.; Cui, Q.; Baboul, A. G.; Clifford, S.; Cioslowski, J.; Stefanov, B. B.; Liu, G.; Liashenko, A.; Piskorz, P.; Komaromi, I.; Martin, R. L.; Fox, D. J.; Keith, T.; Al-Laham, M. A.; Peng, C. Y.; Nanayakkara, A.; Challacombe, M.; Gill, P. M. W.; Johnson, B.; Chen, W.; Wong, M. W.; Gonzalez, C.; Pople, J. A. *Gaussian 03*, revision C.02; Gaussian, Inc.: Wallingford, CT, 2004.

(20) Becke, A. D. *Phys. Rev. A* **1988**, *38*, 3098−3100. (b) Lee, C.; Yang, W.; Parr, R. G. *Phys. Rev. B* **1988**, *37*, 785−789. (c) Becke, A. D. *J. Chem. Phys.* **1993**, *98*, 5648−5652.

(21) Hemelsoet, K.; Moran, D.; Van Speybroeck, V.; Waroquier, M.; Radom, L. *J. Phys. Chem. A* **2006**, *110*, 8942−8951.

(22) (a) Gomez-Balderas, R.; Coote, M. L.; Henry, D. J.; Radom, L. *J. Phys. Chem. A* **2004**, *108*, 2874−2883. (b) Coote, M. L. *J. Phys. Chem. A* **2004**, *108*, 3865−3872.

(23) Boese, A. D.; Martin, J. M. L. *J. Chem. Phys.* **2004**, *121*, 3405−3416.

(24) (a) Wood, G. P. F.; Rauk, A.; Radom, L. *J. Chem. Theory Comput.* **2005**, *1*, 889−899. (b) Miller, D. J. Smith, D. M.; Chan, B.; Radom, L. *Mol. Phys.* **2006**, *104*, 777−794. (c) Wood, G. P. F.; Moran, D.; Jacob, R.; Radom, L. *J. Phys. Chem. A* **2005**, *109*, 6318−6325. (d) Hemelsoet, K.; Moran, D.; Van Speybroeck, V.; Waroquier, M.; Radom, L. *J. Phys. Chem. A* **2006**, *110*, 8942−8951.

(25) (a) Van Speybroeck, V.; Van Neck, D.; Waroquier, M.; Wauters, S.; Saeys, M.; Marin, G. B. *J. Phys. Chem. A* **2000**, *104* (46), 10939−10950. (b) Vansteenkiste, P.; Van Speybroeck, V.; Marin, G. B.; Waroquier, M. *J. Phys. Chem. A* **2003**, *107* (17), 3139−3145 (c) Van Speybroeck, V.; Vansteenkiste, P.; Van Neck, D.; Waroquier, M. *Chem. Phys. Lett.* **2005**, *402*, 479−484.

(26) Van Cauter, K.; Van Speybroeck, V.; Vansteenkiste, P.; Reyniers, M. F.; Waroquier, M. *ChemPhysChem* **2006**, *7* (1), 131−140.

(27) Morrison, D. A.; Davis, T. P. *Macromol. Chem. Phys.* **2000**, *201*, 2128−2137.

(28) De La Rosa, A.; Heux, L.; Cavaille, J. Y.; Mazeau, K. *Polymer* **2002**, *43*, 5665−5677.

(29) Fischer, H.; Radom, L. *Angew. Chem., Int. Ed.* **2001**, *40*, 1340−1371.

(30) Zammit, M. D.; Coote, M. L.; Davis, T. P.; Willett, G. D. *Macromolecules* **1998**, *31*, 955−963.

(31) (a) Troe, J. *Chem. Rev.* **2003**, *103*, 4565. (b) Wardlaw, D. W.; Marcus, R. A. *Adv. Chem. Phys.* **1988**, *70* (Part 1), 231. (c) Klippenstein, S. J., In *Chemical Dynamics and Kinetics of Small Radicals*; Liu, K., Wagner, A. F., Eds.; World Scientific: Singapore, 1995; Part 1, p 120. (d) Truhlar, D. G.; Garrett, B. C.; Klippenstein, S. J. *J. Phys. Chem.* **1996**, *100*, 12771−12800. (e) Hase, W. L. *Acc. Chem. Res.* **1983**, *16*, 258.

(32) Klippenstein, S. J.; Georgievskii, Y.; Harding, L. B. *Phys. Chem. Chem. Phys.* **2006**, *8*, 1133−1147.

(33) (a) Tomasi, J.; Mennucci, B.; Cancès, E. *J. Mol. Struct.: THEOCHEM* **1999**, *464*, 211. (b) Cancès, M. T.; Mennucci, B.; Tomasi, J. *J. Chem. Phys.* **1997**, *107*, 3032. (c) Mennucci, B. Tomasi, J. *J. Chem. Phys.* **1997**, *106*, 5151. (d) Mennucci, B.; Cancès, E.; Tomasi, J. *J. Phys. Chem. B* **1997**, *101*, 10506.

(34) Eckart, C. *Phys. Rev.* **1930**, *35*, 1303.

(35) Wigner, E. Z. *Phys. Chem. B* **1932**, *19*, 203.

MA071106I